30 Apr 1981, 1:30 pm - 5:30 pm

Analysis of Dynamic Shear Strain Distributed in Three Dimensional Earthdam Models

T. Ohmachi

Tokyo Institute of Technology, Japan

Proceedings: First International Conference on Recent Advances in Geotechnical Earthquake Engineering and Soil Dynamics, April 26 - May 3, 1981, St. Louis, Missouri

Analysis of Dynamic Shear Strain Distributed in Three Dimensional Earthdam Models

T. Ohmachi

Associate Professor of Environmental Engineering, Tokyo Institute of Technology, JAPAN

SYNOPSIS Dynamic shear strain distributions have been evaluated and illustrated for three dimensional earthdam models. The analysis method applied here is a simplified finite element method, which has proved to give vibration modes of an earthdam to a satisfactory level of accuracy by involving a smaller number of degrees of freedom. Mass and stiffness matrices of a dam have been formulated for two types of the shear modulus distribution, one uniform and the other linearly increasing with depth below the crest. Both magnitude and location of the maximum shear strain have been discussed in relation to topography of dam sites.

INTRODUCTION

Dynamic analysis for earth structures has been usually performed by two dimensional methods related to vertical transverse cross sections of the structures. This kind of analysis, when applied to embankment dams, will employ such idealizations as plane strain conditions under which the earthquake response of a dam is free from restraint of both abutments on right and left. However, this idealization is not always available in actual cases where the width to height ratio of the dam is not large enough for the restraint effects to be negligible.

Three dimensional finite element analysis may be ideal for analysing performance of a dam excited by earthquake motions. But even for linear elastic problems, the ordinary method formulated by direct application of three dimensional elastic theory involves such a large number of degrees of freedom that it takes too much computational job and tedious work. Recent studies on dynamic behaviors of embankment dams during earthquakes have revealed that the lowest few modes of vibration are generally predominant in the earthquake response. This will imply that higher modes of vibration are less significant, and thus an adequate method involving a smaller number of degrees of freedom could be developed for the practical purposes.

From this point of view, the author has recently proposed a simplified procedure to evaluate three dimensional vibration modes of an earthdam. This paper describes dynamic shear strain distributions for earthdam models predicted by the procedure as well as the outlines of the formulation and the solution accuracy details of which can be seen in references 1) and 2).

FORMULATION OF THE PROCEDURE

Basic Equations

The stress at a point in an earthdam subjected to earthquake excitation could be conveniently expressed as the sum of the static stress plus the additional dynamic stress induced by the dynamic forces. The first step to evaluate the three dimensional dynamic stress is to derive the equations of motion of the dam during the undamped free vibration.

Let us take x coordinate parallel to the dam axis, y coordinate in the upstream-downstream direction and z vertically downward. Displacement components in each direction will be expressed by u, v and w, respectively. To simplify the formulation, we introduce an assumption that the shear stress distribution is uniform in y direction. Hence, the displacements u and w should be

$$\frac{\partial u}{\partial y} = \frac{\partial w}{\partial y} = 0 \tag{1}$$

Consider an infinitely small fiber element with a rectangular cross section (dx x dz) directing transversely to the dam axis, as shown in Fig.1. Stress components acting on the element surface is listed in TABLE I, in which σ denotes normal stress and τ shear stress. By d'Alembert's principle,dynamic equilibrium in each direction can be expressed in the form

$$\frac{\partial^2 u}{\partial t^2} = -\frac{1}{\rho}\left(\frac{1}{z}\tau_{zx} + \frac{\partial \tau_{zx}}{\partial z} + \frac{\partial \sigma_x}{\partial z}\right) \tag{2a}$$

$$\frac{\partial^2 v}{\partial t^2} = -\frac{1}{\rho}\left(\frac{1}{z}\tau_{zy} + \frac{\partial \tau_{zy}}{\partial z} + \frac{\partial \tau_{xy}}{\partial x}\right) \tag{2b}$$

$$\frac{\partial^2 w}{\partial t^2} = -\frac{1}{\rho}\left(\frac{1}{z}\sigma_z + \frac{\partial \sigma_z}{\partial z} + \frac{\partial \tau_{xz}}{\partial x}\right) \tag{2c}$$

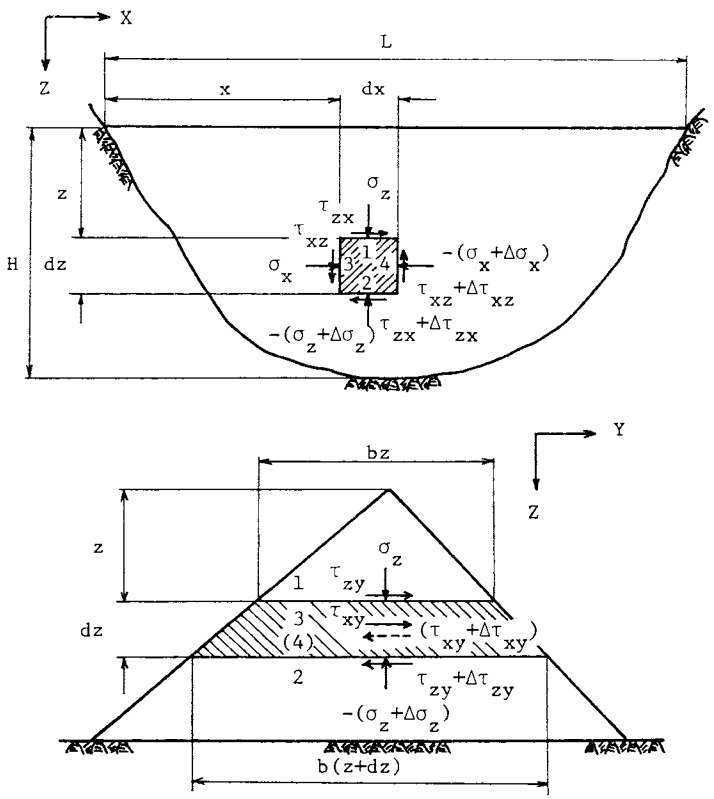

Fig. 1. Stresses on a Rectangular Fiber Element

TABLE I. Stresses in Each Direction

Id. No.	Area	Stress Components in each direction		
		x	y	z
1	bz·dx	τ_{zx}	τ_{zy}	σ_z
2	b(z+dz)dx	$-(\tau_{zx}+\frac{\partial\tau_{zx}}{\partial z}dz)$	$-(\tau_{zy}+\frac{\partial\tau_{zy}}{\partial z}dz)$	$-(\sigma_z+\frac{\partial\sigma_z}{\partial z}dz)$
3	$b(z+\frac{dz}{2})dz$	σ_x	τ_{xy}	τ_{xz}
4	$b(z+\frac{dz}{2})dz$	$-(\sigma_x+\frac{\partial\sigma_x}{\partial x}dx)$	$-(\tau_{xy}+\frac{\partial\tau_{xy}}{\partial x}dx)$	$-(\tau_{xz}+\frac{\partial\tau_{xz}}{\partial x}dx)$

In Eqs.(2), t denotes time and ρ mass density of the dam material.

As for dynamic stability of an embankment dam, horizontal motion in the upstream-downstream direction will be most important. This paper is to illustrate the strain induced by this motion. From the first assumption in Eq.(1), the shear stresses in Eqs.(2) becomes

$$\tau_{xy} = G\gamma_{xy} = G\frac{\partial v}{\partial x} \tag{3a}$$

$$\tau_{yz} = G\gamma_{yz} = G\frac{\partial v}{\partial z} \tag{3b}$$

in which G denotes shear modulus. Substituting Eqs.(3) into Eq.(2b) leads

$$\frac{\partial^2 v}{\partial t^2} = C_s^2\left(\frac{\partial^2 v}{\partial x^2} + \frac{1}{z}\frac{\partial v}{\partial z} + \frac{\partial^2 v}{\partial z^2}\right) \tag{4}$$

in which

$$C_s = \sqrt{G/\rho} \quad \text{(shear wave velocity)} \tag{5}$$

Hatanaka[3] solved the differential equation for the simplest case where the dam is modeled by a uniform shear wedge beam as shown in Fig.2. The solution satisfying the boundary conditions, i.e., v=0 at x=0, v=0 at x=L, v=0 at z=H, and dv/dz=0 at z=0, is written in the form

$$v(x,z,t) = \sum_n^{\infty} A_n \exp(ipt)g(x,z) \tag{6a}$$

$$g(x,z) = \sin\frac{n\pi x}{L} J_0\left(\frac{z_m z}{H}\right) \tag{6b}$$

in which i represents imaginary unit, J_0 Bessel function of first kind and order zero, and z_m the zero value of the frequency equation $J_0(pH/C_s)=0$ having a fixed value for each mode in the x-z plane as listed in TABLE II. The natural circular frequency p in Eq.(6a) is given in dimensionless form when multiplied by the height and devided by the shear wave velocity

$$pH/C_s = \sqrt{z_m^2 + n^2\pi^2(H/L)^2} \tag{8}$$

in which n represents the number of the mode in the x-y plane.

It should be noted that the solution in Eqs.(6) is well separated with respect to each variable and that the modal shape function g(x,z) is represented as the product of each appropriate function of x and z. This is a simple statement of the basic concepts employed in the following formulation and analyses.

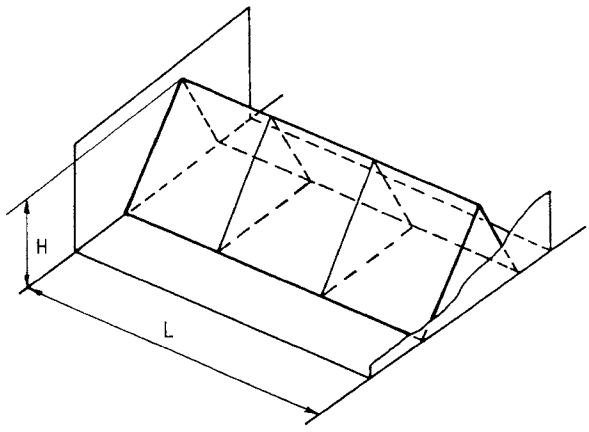

Fig. 2. Earthdam Model in a Rectangular Canyon

Application of Finite Element Technique

The finite element analysis technique[4] has been used to formulate such dynamic properties as mass and stiffness matrices of an earthdam. Consider a prismatic finite element which is obtained by deviding a dam model with vertical transverse planes, as shown in Fig.3. To express the modal shape function of v(x,z,t), newly defined notation v(x,z) will be used in the following. When a linear interpolation function is introduced to express the translational displacement along the crest, the displacement on the crest of the element v(x,0) will be

$$v(x,0) = SCV \tag{9}$$

in which

$$S = [\ 1 \quad x\ ] \tag{10}$$

$$C = \begin{bmatrix} 1 & 1 \\ 1/\ell & 1/\ell \end{bmatrix} \tag{11}$$

$$V = [\ v_i \quad v_j\ ]^T \tag{12}$$

In the above equations, ℓ is the element length along the crest, V denotes the nodal crest displacement vector, and T means the transpose. From the assumption written by Eq.(4), the displacement at any point of the element will be given by

$$v(x,z) = v(x,0)f(x,z) \tag{13}$$

in which the vibrating shape function in the x-z plane f(x,z) should be

$$f(x,0) = 1 \tag{14a}$$

$$f(x,H_x) = 0 \tag{14b}$$

where

$$H_x = H_i + (H_j - H_i)x/\ell \tag{14c}$$

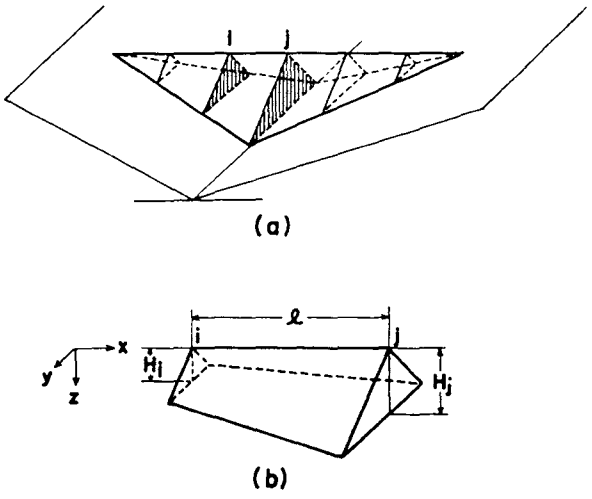

Fig. 3. Finite Element Idealization

In Eq.(14b), H_x denotes the sectional height of the element.

Shear strains related to v(x,z) are, from Eqs.(3) and (9)-(13)

$$[\ \gamma_{xy} \quad \gamma_{yz}\ ]^T = BCV \tag{15}$$

in which

$$B = \begin{bmatrix} f_x(x,z) & f(x,z)+xf_x(x,z) \\ f_z(x,z) & xf_z(x,z) \end{bmatrix} \tag{16}$$

$$f_x(x,z) = \partial f/\partial x, \quad f_z(x,z) = \partial f/\partial z \tag{17}$$

Thus, the stiffness matrix of the element can be evaluated by the following volume integration

$$k = \int_v C^T B^T D B C \ d(vol) \tag{18}$$

$$D = \begin{bmatrix} G & 0 \\ 0 & G \end{bmatrix} \tag{19}$$

The matrix product in Eq.(18) can be expanded to

$$B^T D B = G\{f^2(x,z)N^T N + f(x,z)f_x(x,z)(N^T S + S^T N) + f_x^2(x,z)S^T S + f_z^2(x,z)S^T S\} \tag{20}$$

$$N = [\ 0 \quad 1\ ] \tag{21}$$

Substituting Eq.(20) into Eq.(18) and integrating termwise will serve to express the stiffness matrix as the sum of four submatrices

$$k = k_1 + k_2 + k_3 + k_4 \tag{22}$$

The mass matrix of the element can be similarly evaluated by

$$m = \int_v f^2(x,z)\rho C^T S^T S C \ d(vol) \tag{23}$$

TABLE II Examples of Shape Function

Shear Modulus Distribution	G=G(const.)	$G=G_0 z$
Shape Function in x-z Plane f(x,z)	$J_0(\zeta)$ where $\zeta=\frac{z_m z}{H_x}$	$\frac{2}{\sqrt{\zeta}}J_1(\sqrt{\zeta})$
Z_m values and Shapes of f(x,z)=0	z_1 2.405 crest z_2 5.520 z_3 8.654 2nd mode 1st mode bottom	14.68 crest 49.22 103.50 2nd mode 1st mode bottom

Mass and Stiffness Matrices

Introducing an appropriate function for f(x,z) and conducting integration given by Eqs.(18) and (23) provide concrete forms of stiffness and mass matrices. The matrices are exemplified for two types of earthdam models shown in TABLE II, in which the shape function can be found in the second row. The function in terms of Bessel function of order zero is for a model having a uniform shear modulus, and that of order one is for a model having a shear modulus linearly increasing with depth below the crest.

a) For a model with $G=G$ (const.) and $\rho=\rho$ (const.)

$$k_1 = G\eta(H_i^2+H_j^2+H_iH_j)/\ell^2\begin{bmatrix}2 & -2\\ -2 & 2\end{bmatrix} \tag{24}$$

$$k_2 = G\eta/\ell^2\begin{bmatrix}2(2H_i^2-H_iH_j-H_j^2) & (2H_iH_j-H_i^2-H_j^2)\\ (2H_iH_j-H_i^2-H_j^2) & 2(2H_j^2-H_iH_j-H_i^2)\end{bmatrix} \tag{25}$$

$$k_3 = G\eta(4+z_m^2)(H_j-H_i)^2/\ell^2\begin{bmatrix}2/3 & 1/3\\ 1/3 & 2/3\end{bmatrix} \tag{26}$$

$$k_4 = G\eta z_m^2\begin{bmatrix}2 & 1\\ 1 & 2\end{bmatrix} \tag{27}$$

$$m = \rho\eta\begin{bmatrix}(6H_i^2+H_j^2+3H_iH_j)/5 & (3H_i^2+3H_j^2+4H_iH_j)/10\\ (3H_i^2+3H_j^2+4H_iH_j)/10 & (H_i^2+6H_j^2+3H_iH_j)/5\end{bmatrix} \tag{28}$$

in which

$$\eta = b\ell J_1^2(z_m)/12 \tag{29}$$

b) For a model with $G=G_0z$ and $\rho=\rho$ (const.)

$$k_1 = 20G_0\eta(H_i^3+H_i^2H_j+H_iH_j^2+H_j^3)\begin{bmatrix}1 & -1\\ -1 & 1\end{bmatrix} \tag{30}$$

$$k_2 = 20G_0\eta(H_i-H_j)\begin{bmatrix}3H_i^2+H_j^2+2H_iH_j & -(H_i^2-H_j^2)\\ -(H_i^2-H_j^2) & -(H_i^2+3H_j^2+2H_iH_j)\end{bmatrix} \tag{31}$$

$$k_3 = G_0\eta(z_m+16)(H_i-H_j)^2\begin{bmatrix}3H_i+H_j & H_i+H_j\\ H_i+H_j & H_i+3H_j\end{bmatrix} \tag{32}$$

$$k_4 = 5G_0\eta\ell^2z_m\begin{bmatrix}3H_i+H_j & H_i+H_j\\ H_i+H_j & H_i+3H_j\end{bmatrix} \tag{33}$$

$$m = 4\rho\eta\ell^2\begin{bmatrix}2(6H_i^2+H_j^2+3H_iH_j) & 3H_i^2+3H_j^2+4H_iH_j\\ 3H_i^2+3H_j^2+4H_iH_j & 2(H_i^2+6H_j^2+3H_iH_j)\end{bmatrix} \tag{34}$$

in which

$$\eta = bJ_0^2(\sqrt{z}_m)/60\ell z_m \tag{35}$$

The matrices for the complete structure made up of these element matrices have a tridiagonal form.

Comparison of Solutions

To examine the accuracy of the procedure formulated above, comparison is made to the undamped natural frequencies of homogeneous earthdam models in a rectangular canyon.

Frazier[5] evaluated vibration modes of the models by the ordinary three dimensional finite element method. He used tetrahedral elements having movable nodes located at the third points along the length as shown in Fig.2. The number of degrees of freedom involved in his analysis is 90, and side slopes of the models being symmetric with respect to the axis are 1:1.5 and 1:3.0.

The values in the lowest row in each column of TABLE III are solutions of the eigenproblem which consists of mass and stiffness matrices given by Eqs.(22)-(29), computed by involving 19 degrees of freedom. The modal shapes and the location of movable nodes are shown in the upper part of Fig.4.

TABLE III Computed Natural Circular Frequencies Represented in Dimensionless Form pH/C_s

Mode Descr* m	Mode Descr* n	Comp. Proc.**	Length to Height Ratio L/H: 1	2	5	10	∞	ν***
1	1	3-D 1:1.5	3.80	2.81	2.47	2.42	(2.33)	.45
		3-D 1:3.0	3.68	2.65	2.28	2.22	(2.15)	〃
		S-W Rigor.	3.96	2.87	2.49	2.43	2.40	
		S-W F.E.M.	3.96	2.87	2.49	2.43	2.40	
1	2	3-D 1:1.5	5.67	3.57	2.74	2.60	(2.33)	.45
		3-D 1:3.0	5.57	3.40	2.48	2.33	(2.15)	〃
		S-W Rigor.	6.73	3.96	2.71	2.49	2.40	
		S-W F.E.M.	6.75	3.97	2.72	2.49	2.40	
2	1	3-D 1:1.5	6.85	6.41	5.69	5.10	(5.79)	.45
		3-D 1:3.0	5.32	4.72	4.60	4.56	(4.73)	〃
		S-W Rigor.	6.35	5.74	5.56	5.53	5.52	
		S-W F.E.M.	6.35	5.74	5.56	5.53	5.52	

* m and n represent the number of modes along the height and length, respectively.

** The computing procedures include Three-Dimensional F.E.M.(3-D) together with Plane-Strain Solution in parenthesis, and Shear-Wedge Solution given by Eq.(8)(S-W.Rigor.) and that given by Eqs.(22)-(29)(S-W.F.E.M.).

*** Poisson's ratio used in Frazier's analysis.

From TABLE III, it could be pointed out that this numerical procedure provides vibration modes accurate enough for the practical purposes by involving a smaller number of degrees of freedom. Besides being simple, this procedure gives such a smooth mode shape along the length that it can serve to evaluate continuous strain distribution in the model.

The natural frequencies for a model in a V-shaped canyon are shown at the right side of Figs.5 and 6 in the same manner as in TABLE III. It is evident that these frequencies are almost two times as high as those for a model in a rectangular canyon, due to the stronger restraint of the canyon wall.

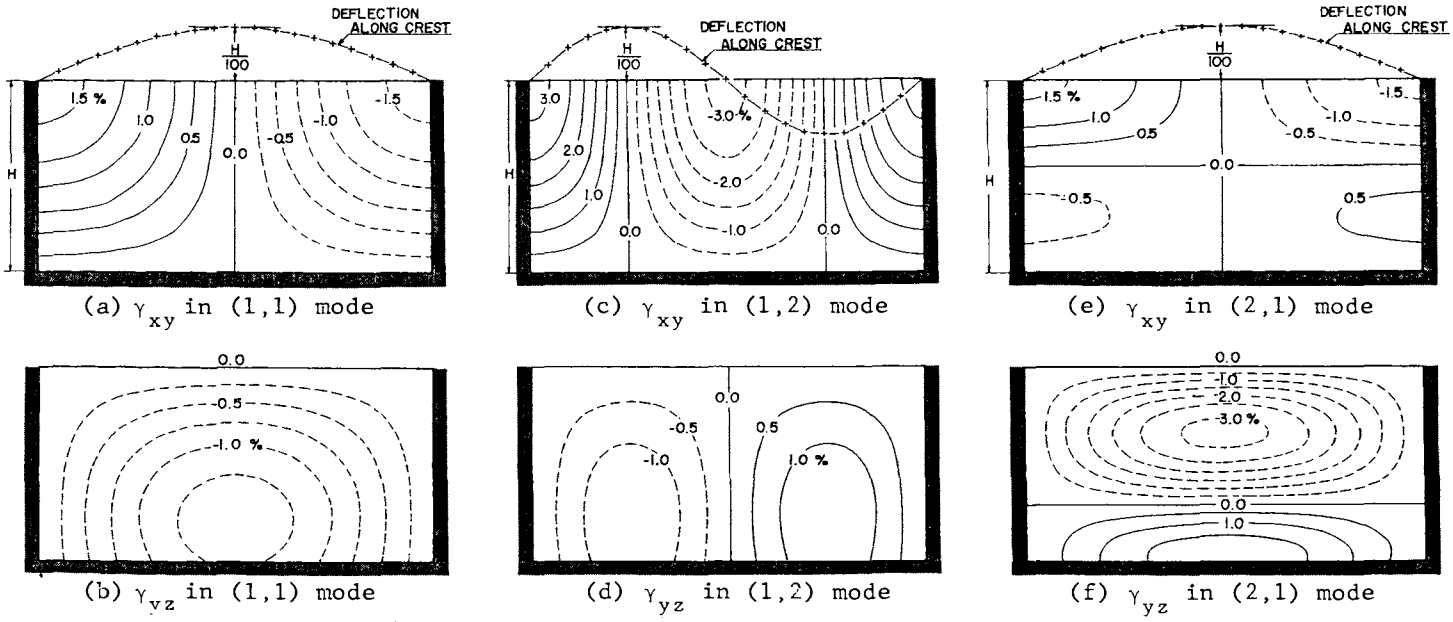

(a) γ_{xy} in (1,1) mode (c) γ_{xy} in (1,2) mode (e) γ_{xy} in (2,1) mode

(b) γ_{yz} in (1,1) mode (d) γ_{yz} in (1,2) mode (f) γ_{yz} in (2,1) mode

Fig.4 Dynamic Shear Strain of a Dam with a Uniform Shear Modulus in a Rectangular Canyon(L/H=2)

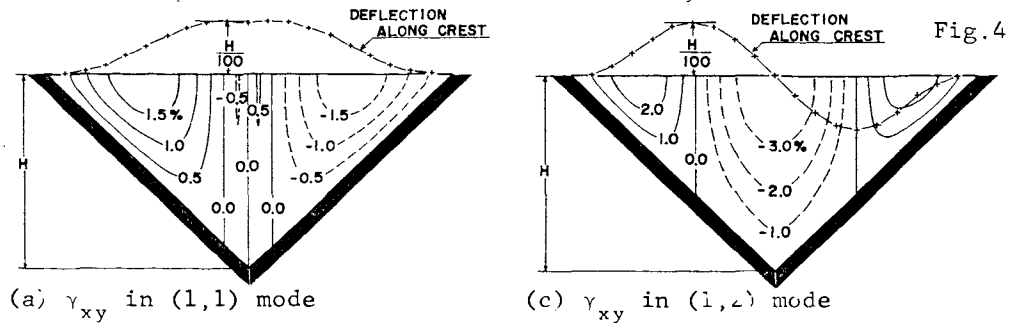

(a) γ_{xy} in (1,1) mode (c) γ_{xy} in (1,2) mode

L/H = 2

pH/C_s = 4.30 for (1,1) mode
6.25 for (1,2) mode

Slope of Canyon Wall
1:1.0 (right bank)
1:1.0 (left bank)

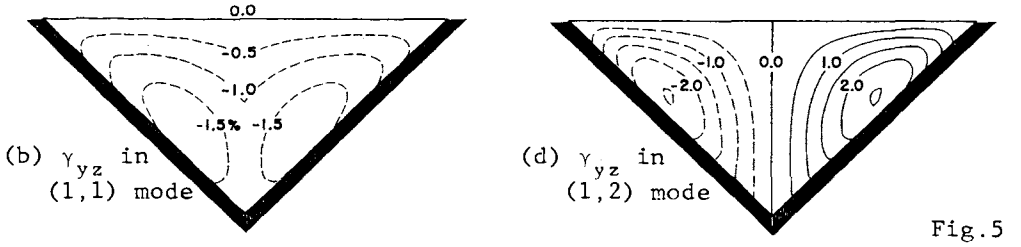

(b) γ_{yz} in (1,1) mode (d) γ_{yz} in (1,2) mode

Fig.5 Dynamic Shear Strain of a Dam with a Uniform Shear Modulus in a Symmetric V-shaped Canyon

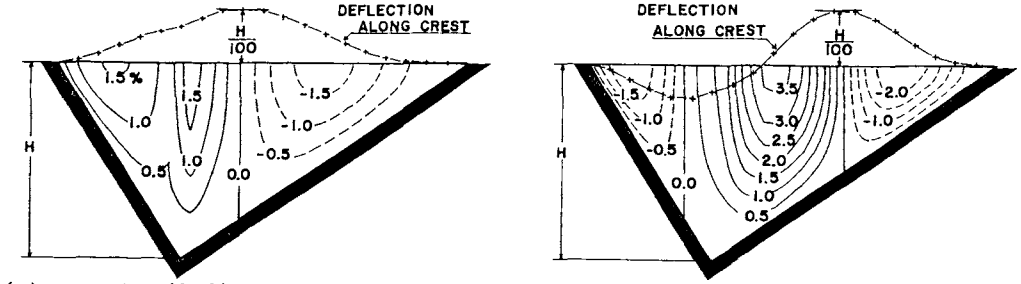

(a) γ_{xy} in (1,1) mode (c) γ_{xy} in (1,2) mode

L/H = 2

pH/C_s = 4.32 for (1,1) mode
6.29 for (1,2) mode

Slope of Canyon Wall
1:1.2 (right bank)
1:0.8 (left bank)

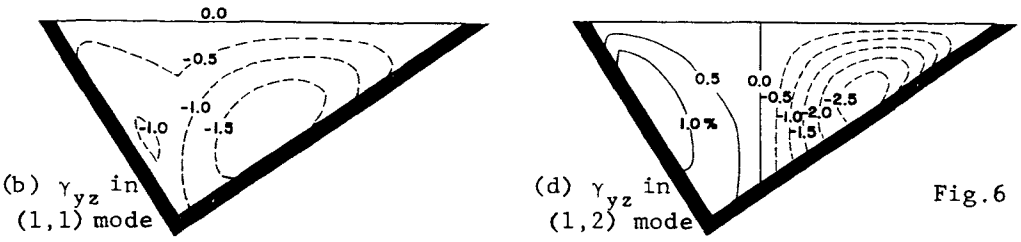

(b) γ_{yz} in (1,1) mode (d) γ_{yz} in (1,2) mode

Fig.6 Dynamic Shear Strain of a Dam with a Uniform Shear Modulus in an Asymmetric V-shaped Canyon

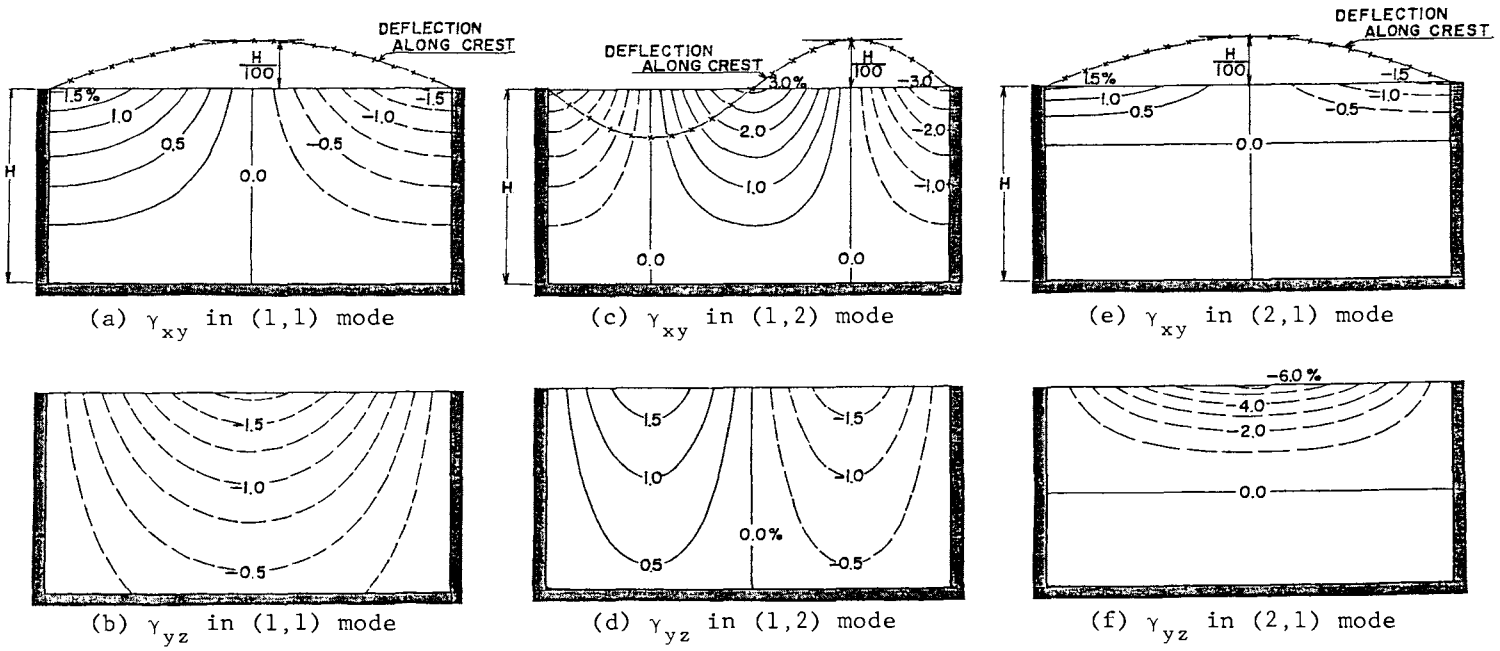

(a) γ_{xy} in (1,1) mode (c) γ_{xy} in (1,2) mode (e) γ_{xy} in (2,1) mode

(b) γ_{yz} in (1,1) mode (d) γ_{yz} in (1,2) mode (f) γ_{yz} in (2,1) mode

Fig.7 Dynamic Shear Strain of a Dam with $G=G_0z$ in a Rectangular Canyon

DYNAMIC SHEAR STRAIN

For the lowest two or three modes of vibration, shear strain distributions are shown in Figs.4-7, in which all the maximum modal displacements are normalized to be 1 % of the dam height.

When a shear modulus is uniformly distributed in a dam, the maximum of γ_{xy} developes along the crest surface, while the maximum of γ_{yz} developes deep inside the dam. As far as the lowest mode for L/H=2 is concerned, these maximum values are roughly equal each other, despite of variation in the canyon shape. But the location of high value of γ_{xy} approaches the midspan of the crest as the canyon slope becomes gentler.

The (1,2) mode of vibration will hardly appear in a symmetric dam with a rigid foundation. But in an asymmetric dam, this mode will readily appear and induce a larger strain than can be estimated by conventional two-dimensional analyses. Another effect of asymmetry in canyon shape lies in the fact that the additional high strain area of γ_{xy} developes around the deepest section where the vibrating shape changes abruptly, as shown in Fig.6(a).

For a shear modulus increasing with depth below the crest, the distribution of γ_{yz} is quite different from that for a uniform shear modulus while the difference is less with respect to γ_{xy}. That is, a large value of γ_{yz} developes also along the crest surface, and the maximum of γ_{yz} is evidently larger than that of γ_{xy}. It should be noted that multiplying the shear strain shown in Fig.7 by G_0z results in the maximum shear stress developing at the midheight of the dam.

CONCLUDING REMARKS

In a word, the procedure described here is an extension of the shear-wedge theory with the application of the finte element method. This procedure enables to obtain vibration modes of a three dimensional earthdam by involving such a small number of degrees of freedom that the natural frequencies and vibration mode shapes could be evaluated by hand calculation.

Little attention has been paid to the dynamic shear strain induced by the difference in vibration displacement along the length of an earthdam. But this kind of strain mainly developes along the crest surface, and in usual cases the magnitude will be of significant level to the stability of the dam. Especially for a dam in an asymmetric canyon, the stress relating to the strain is likely to become of great importance.

REFERENCES

1) Ohmachi,T.(1980):A Practical Solution for Evaluating Three Dimensional Vibraion Modes of an Earthdam, Tech.Report No.26, pp.125-136, Dept.Civ.Engrg.,Tokyo Inst.Tech., Japan.
2) Ohmachi,T. et al.(1980):Vibration Analyses of Three Dimensional Earthdams by the Finite Shear-Wedge Model (to be published).
3) Hatanaka,M.(1952):Three Dimensional Consideration on the Vibration of Earth Dams, Jour. JSCE, 37-10, pp.1-6, Tokyo, Japan.
4) Zienkiewicz,O.C.& Y.K.Cheung(1967):The Finite Element Method in Structural and Continuum Mechanics, McGraw Hill, New York, N.Y.
5) Frazier,G.A.(1969):Vibration Characteristics of Three Dimensional Solids with Application to Earth Dams, ph.D. Thesis Submitted to Montana State Univ.,Montana.